

On Measurement Models for Line Segments and Point Based SLAM

Satish Pedduri, Gururaj Kosuru, K Madhava Krishna and Amit K Pandey*

†

Abstract

We present efficient measurement models for localization in a feature based EKF SLAM framework. Both points and segments form the features, points include corners formed by intersection of wall like segments. The point features are described by its coordinates, while the segment feature is represented by the angle made by the normal to the segment from the global origin with the abscissa called the normal angle or N-angle for short. The measurement equation involves measuring the distance and bearing to the point feature and only bearing to the line feature. The distance measurement to the segment is intentionally kept out of the measurement equation due to its inefficacy in correcting the robot and landmarks state. This arises due to very large differences in the predicted and observed distances even for modest measurement errors when the robot is not very near the segment. Hence for this reason the segment feature is represented only by its N-angle devoid of distance since such a representation results in better state correction. The number of computations resulting from the covariance matrix updates is also less than a representation that includes both N-distance and N-angle.

1. INTRODUCTION

The SLAM problem has witnessed immense attention from the robotic community. There are now many excellent material to initiate the reader in a systematic fashion [1, 2, 3]. Several solutions have been proposed that include the popular Extended Kalman Filter framework [4], the FAST-SLAM framework which uses EKF to model the map features while a set of particles describe the probable robot trajectories [5] and the Graph SLAM [6]. Within the EKF framework there have been many approaches that have tried to keep a check on the growth of the covariance matrix for real-time considerations. For example in [7] a

compressed EKF (CEKF) is proposed that updates only part of the map one can see while the rest of the update is postponed. A faster alternative to the EKF based on factorization of the information matrix was proposed in [8]. Others have attacked the problem of improving the data association, which is very crucial for a successful SLAM implementation using methods such as joint compatibility branch and bound [10], the Maximal Common Subgraph [9] and the combined constrained data association [11].

In this paper the concern is about approaches that use both point and segment features as landmarks. The amount of literature on segment based EKF SLAM has been relatively sparse. In a recent paper [12] a line feature based SLAM with lower end sensors such as an IR range finder was proposed. The paper formulates the framework for segments that are parallel to one of the two axes of the global reference frame. In [13] the line feature is represented by its center of gravity. By tracking corners that form the endpoints of the line the statistical growth of line like features is curtailed. Earlier a framework of SLAM based on segment representation and map management was presented in [14]. However this work did not consider incorporating point features also as part of the landmarks.

This paper draws certain inferences in the context of segment and point features based EKF SLAM that has not appeared before in other literature based on our survey. Firstly it infers that a measurement equation involving the normal distance or any such distance measure to a line feature is highly sensitive to even modest measurement noise. Thus even the initial features augmented to the state matrix possess very high variance and covariances. These high values prevent subsequent correction of the state vector. Secondly the measurement equation involving N-angle to the line feature is a lot more stable to measurement noise and hence can correct the state vector closer to its actual value. Thirdly the bearing measurement of point features is more sensitive to measurement noise when the robot is close to the feature than the n-angle measurement to the line feature. Based on these inferences the paper shows the following:

1. Including line features apart from point features with only n-angle being measured in line features results

*Satish is a research assistant and Gururaj is a graduate students at the Robotics Research Center, IIIT Hyderabad while K Madhava Krishna is a faculty at the same center

†Amit K Pandey is with Robotics and AI group, LAAS-CNRS, Toulouse, France

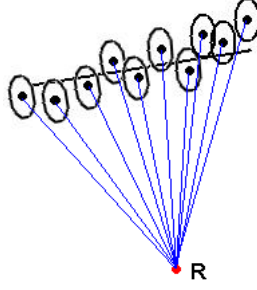


Figure 1: Figure depicting set of points measured with a ranger device like laser. Associated ellipses around each point are uncertainties.

in more robust state correction than using only point features.

2. Involving N-distance in the measurement as well as a landmark feature does not improve the state correction at all or rather inconsequentially. Sometimes it is found to degrade the performance. Hence with only N-angle in the measurement and representation of the feature leads to better performance than having both n-distances and n-angles, when the option exists to get distance measurement from points.

While decomposing the line feature to a point through its center of gravity as described in [13] could alleviate some of the issues described above, it is a difficult proposition to track the center of gravity when the line is not completely seen and the length of the line varies from scan to scan.

2. Motivation

We elaborate the inferences mentioned through figures that constitute our motivation. Figure 1 shows a set of points as measured by a range device like the Laser Range Finder (LRF) that constitutes a segment like object such as a wall. The uncertainty ellipses of these points are also shown. The uncertainties in the laser range measurement and the uncertainty of the angle of the laser ray are transformed to the uncertainties in the coordinates of the measured point and shown by the ellipses. We are not depicting uncertainty in the robot pose for the time being for the sake of clarity in these illustrations. Consider two probable line segments that could arise due to these uncertainties shown in blue and green in figure 2. We regard the blue line to be the predicted line segment and the green as the obtained or perceived line from the most recent scan. The perpendiculars to these two line segments are shown from two different robot positions. Evidently the difference between the perpendicular distance to the two lines is rather

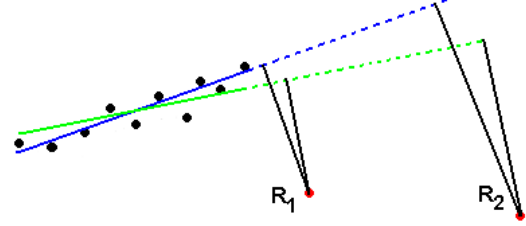


Figure 2: Perpendicular distances dropped from two robot locations (R_1, R_2) to predicted line(blue) and perceived line(green). Clearly the difference between perpendicular distances from location R_2 is more than the difference from location R_1 .

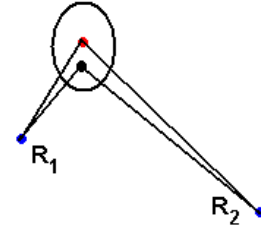


Figure 3: The distances drawn from Robot locations (R_1, R_2) to the predicted and perceived points. Depending on the robot's location, the difference between distances to predicted and perceived points is bounded inside the ellipse.

large and it grows as the distance of the robot from the segment increases. These large differences in the predicted and obtained measurements results in large variance terms for the distance measurement essentially rendering the perpendicular distance ineffective for state error correction or update. A bit more formally if $X_r = [x_r, y_r, \theta_r]^T$ represents the robot state and $X_l = [x_l, y_l]^T$ any point on the segment then the N-distance from the robot to the segment is given by $\rho = x_r \cos(\phi) + y_r \sin(\phi) - \rho_0$, where ϕ is the N-angle to the line and ρ_0 is the N-distance to the line from the origin. If m_l denotes the slope of the line, then the sensitivity of the N-distance from the robot location to the line's slope is given by $\frac{\partial \rho}{\partial m_l} = \frac{1}{1+m_l^2} (x_l - x_r) \sin(\phi) + (y_r - y_l) \cos(\phi)$. Thus the changes in ρ due to changes in m_l gets more pronounced as the robot is further away from the line verifying the observations of figure 2. On the other hand the sensitivity of the bearing to the line, given by $\psi = \phi - \theta_r$, to changes in line slope is of the form $\frac{\partial \psi}{\partial m_l} = \frac{1}{1+m_l^2}$ which is invariant to the distance from the robot to the line.

In case of point features there is no such thing as slope and sensitivity of measurement parameters to slope changes does not arise. However one can discern the sensitivity of point measurement parameters to robot pose due to measurement noise. Figure 3 shows that unlike line features, the difference between predicted and observed distance to a point feature lies within the same bounds of un-

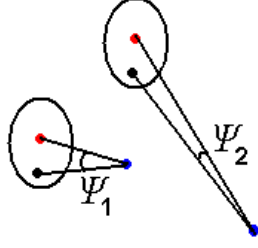


Figure 4: The angle Predicted-Robot-Perceived $\angle PRP$ can greatly vary depending on the robots location with respect to the points.

certainty, irrespective of distance of the robot to the landmark. This is when the measurement noise of the measuring device does not grow as the distance it measures increases, which is normally true for laser and other range finders for a given range of operation. Whereas figure 4 shows that the difference between predicted and measured angles can increase when the robot gets closer to the point feature despite the feature noise remaining a constant. These observations indicate that the bearing to a line feature and distance to a point feature are apt measurement parameters. A careful combination of these could yield a better set of results as the experimental section reveals.

3. The Method

While the current method holds true for any kind of a mobile robot with range sensors, we assume a robot with a differential drive for the sake of simplicity. In our EKF model, we assume that a set of waypoints are given a priori to the robot. Using the control model, the robot finds the route to the next waypoint in discrete steps, using a linear movement command or a rotation command alternately at each step as required. The rotation is performed alternately to correct the deviation in the heading of the robot due to errors such as drift.

At any time, the state consists of the pose of the robot and the features, both being erroneous. The noise in the robot's pose is modeled using two different Gaussian variables, the variance in linear motion and the variance in heading. When experimenting on the robot, the variances are estimated from several runs of the robot. As the pose of the robot is stored using a Cartesian coordinate system, the noise model needs to be mapped from the noise space to the robot space, as below :

$$X_r = [r \cos \theta_r \quad r \sin \theta_r \quad \theta_r]^T$$

$$G_u = \begin{bmatrix} \frac{\partial X_r}{\partial r} \\ \frac{\partial X_r}{\partial \theta} \end{bmatrix} = \begin{bmatrix} \cos \theta_r & -r \sin \theta_r \\ \sin \theta_r & r \cos \theta_r \\ 0 & 1 \end{bmatrix}$$

$$N_{(x,y)} = G_u \times N_{(T,\theta)} \times G'_u$$

Similarly, the observation model for noise is modeled as Gaussians, as according to the type of the feature. For a point feature, the noise is in terms of the range and the bearing variance and for a line, it is in terms of the variance of the N-angle.

$$R_p = \begin{bmatrix} \sigma_r^2 & 0 \\ 0 & \sigma_\theta^2 \end{bmatrix}$$

$$R_l = [\sigma_\psi^2]$$

The state vector initially consists of the robot pose with new observed features being augmented to the state vector with every scan.

$$X_r = [x_r \quad y_r \quad \theta_r \dots \quad x_p \quad y_p \dots \quad \psi_l \quad \dots]^T$$

As in every EKF framework, we model the measurements with the following measurement equation for points and lines respectively.

$$z_p = \begin{bmatrix} \sqrt{(x_p - x_r)^2 + (y_p - y_r)^2} \\ \tan^{-1}(y_p - y_r / x_p - x_r) - \theta_r \end{bmatrix}$$

$$z_l = [\phi - \theta_r]$$

Initially, the robot takes a scan of the environment followed by the EKF algorithm. The algorithm begins with a move command to the robot, followed by the prediction of the new pose and covariance. A scan of the surroundings is acquired next, from which possible features are extracted for augmenting and/or associating to the state, followed by the updating of the state vector from the associated features. These steps are followed iteratively till the last waypoint is reached.

The features acquired from each measurement are stored in their raw form temporarily (with the robot pose as the origin of the coordinate system). With each new measurement, the last raw form array is transformed by the estimated movement of the robot between the last and the current pose and then compared with the raw observations in the current scan. The observations that are yet not associated are then checked for association using the Mahalanobis distance.

For each line segment feature in the state, endpoints are stored separately and updated out of the EKF framework using simple point projection. The endpoints of each observed line from a scan are then compared to a transformed

Map	Method 1	Method 2	Method 3
1	1.5391	0.32748	0.56607
2	1.3176	0.4120	0.4615
3	0.973	0.32	0.37

Table 1: Average landmark error for three different maps using three different methods (All units are in metres). Method 1 uses point features only, method 2 uses points and N-angles from line segments, and the third method uses both points and lines (with ρ and ψ)

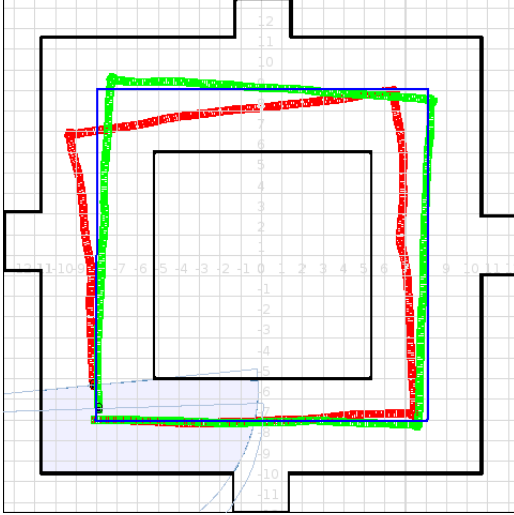


Figure 5: Robot trails for one run of the algorithms. Red trails are when considering point features alone, and green trails using points and N-angles of lines. Whereas the blue lines is the actual path expected. The dimensions of the map are $24 \times 24 m^2$.

set of those obtained from a previous scan stored separately in their original form as obtained. As in the points case, observations that are yet unassociated are then compared with line features from the state for association using endpoints and Mahalanobis distance for the N-angle.

4. Results and Comparisons

Figure 5 shows a map used for simulating our various EKF algorithms. The translation and rotation variances for the differential drive robot used in the simulations were 0.043 metres and 0.02 radians respectively while the laser range and bearing measurement errors were 0.03 metres and 0.017 radians. The variance used for the N-angle of line segment features was 0.03 radians. The ground truth path is shown in the same figure in green, while the mean path obtained by considering only point features is shown in red while the mean path obtained by using point features with both distance and bearing measurements and line features with only bearing measurements is shown in

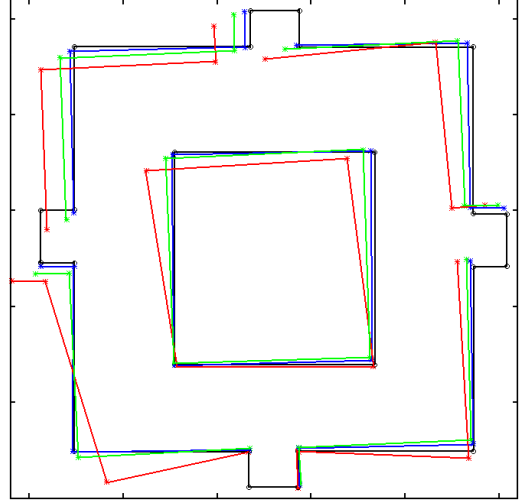


Figure 6: The map estimated by the robot. The map estimated when using points features alone is shown in red, the map estimated with point features and line features (ρ and ψ) is in green, and the map with points and the N-angle of line features is in blue

blue. The figure 6 shows the ground truth map which is same as that of figure 5 in green, the mean values of landmarks when only point features were used in red and when both point and line features were used in blue. These plots indicate that using points and lines as features results in more accurate paths and maps than only point features. The graphs of figure 7 show the error plots of various methods. The abscissa of the plots is the instances when an update of the state was made. The error shows the difference between the ground truth robot state and the mean corrected state at every instant the state update or state correction occurred. The plot in red is due to Method 1 where point features alone used with both bearing and distance measurements. The blue plot corresponds to Method 2 where point features with bearing and distance measurements and line features with only bearing measurements were used. The green plot is of Method 3 where both point and line features had distance and bearing measurements. These plots confirm that Method 2 (points with distance and bearing, lines with only bearing) corrected the robot states much better than Methods 1 and 3. The error in the graph due to point features is quite high in this case due to certain instances where the robot could not see any point features. Although the error might be less in another case it would still be higher than the error incurred when using Method 2.

The graphs of figure 8 have the same connotations as that of figure 7 except they show difference between the ground truth map features and the corrected map features at the end of the navigation run. Every unit on the abscissa corresponds to one iteration of the algorithm, the ordinate is

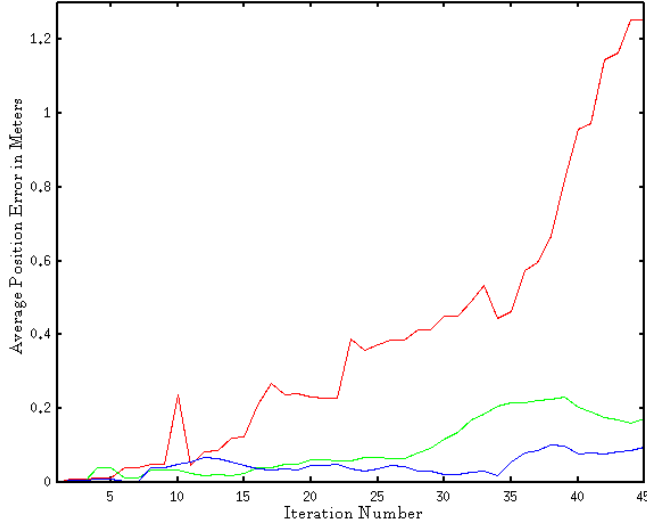


Figure 7: Errors between ground truth and assumed pose. The red graph is for the points only case, the green is for points and lines, and blue is for points and N-angles of lines. The error incurred over a 40 meters movement of the robot is shown.

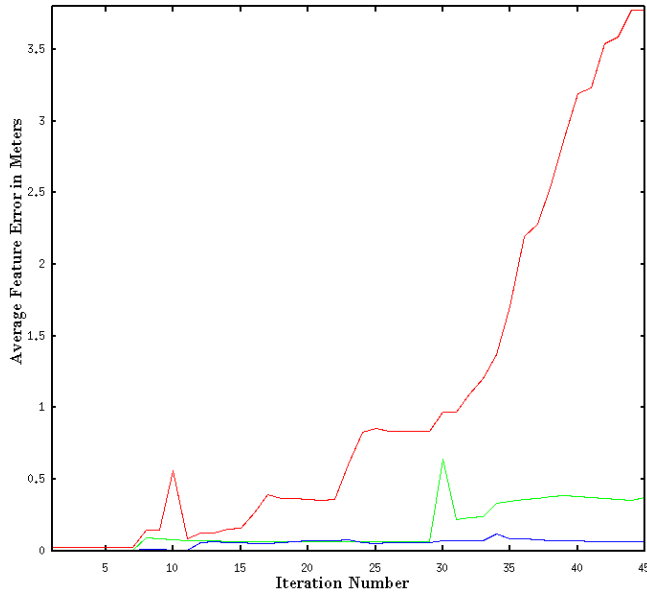


Figure 8: Error between actual feature and estimated feature coordinates. Red for points only, green for points and lines, blue for point and N-angle of lines. The error incurred in features over a 40 meters movement of the robot is shown.

the difference between actual and corrected map feature at the termination of the iteration. Method labels denote the same methods as in the earlier graphs. Once again these confirm the superior performance of Method 2 over 1 and 3.

The experiments have been conducted in simulation environment in Player-Stage, linked to Octave code which was acquired from Tim Bailey's [11] home page and modified to work with the different methods used.

Table 1 tabulates these results in various maps for landmark errors. The first column in the table denotes the various maps across which the comparisons were performed. The remaining columns correspond to methods 1 to 3. The entries in these columns are the average error at the end of the navigation run in that corresponding map. The values in table 1 are the average of the landmark errors (in metres) compared to ground truth. The tabulated results are in consonance with the earlier graphs.

5. Conclusions

The paper makes a case for choosing the apt choice of measurement parameters for a point and segment features based SLAM. The motivation for choosing a particular measurement model stems from the sensitivity of that model with changes in the state of the landmarks that arise due to measurement noise. Those measurement parameters that are less sensitive to changes in state of the landmarks such as slopes in case of segments and position in case of points are preferred over the less sensitive ones. The paper concludes that when the option of using both points and line features exists without any scarcity of those features, a SLAM algorithm that takes only bearing measurements on line and distance and bearing measurements on points performs better than an algorithm that considers only point features or uses both bearing and distance measurements for both lines and point features. Extensive comparisons over various maps corroborate these conclusions

References

- [1] H Durrant Whyte and T Bailey, "SLAM Part 1: The Essential Algorithms" *Robotics and Automation Magazine*, June 2006
- [2] T Bailey and H Durrant Whyte, "SLAM Part 2: The State of the Art" *Robotics and Automation Magazine*, Sep 2006
- [3] S. Thrun, W. Burgard and D. Fox, *Probabilistic Robotics*, MIT Press, 2005
- [4] G. Dissanayake, P. Newman, H.F. Durrant-Whyte, S. Clark, and M. Csoba, "A solution to the simultaneous localisation and mapping (SLAM) problem", *IEEE Trans. Robot. Automat.*, vol. 17, no. 3, pp. 229241, 2001.
- [5] M. Montemerlo, S. Thrun, D. Koller, and B. Wegbreit,

- "Fast-SLAM 2.0: An improved particle filtering algorithm for simultaneous localization and mapping that provably converges", *Proc. Int. Joint Conf. Artif. Intell.*, 2003, pp. 1151-1156.
- [6] J. Folkesson and H.I. Christensen, "Graphical SLAMa self-correcting map", *Proc. IEEE Int. Conf. Robot. Automat (ICRA)*, 2004, pp. 791-798.
 - [7] J. Folkesson and H.I. Christensen, "Outdoor Exploration and SLAM using a Compressed Filter", *Proc. ICRA*, 2003
 - [8] F. Dellaert, "Square Root SAM: Simultaneous location and mapping via square root information smoothing," in *Robotics: Science and Systems (RSS)*, 2005
 - [9] J. Neira and J.D. Tardos, "Robust and feasible data association for simultaneous localization and map building", *In IEEE International Conference on Robotics and Automation*, Workshop on Robot Navigation and Mapping, 2000.
 - [10] J. Neira and J.D. Tardos, "Data association in stochastic mapping using the joint compatibility test", *IEEE Transactions on Robotics and Automation*, 17(6):890-897, 2001
 - [11] T. Bailey, "Mobile robot localisation and mapping in extensive outdoor environments," *Ph.D. dissertation*, Univ. Sydney, Australian Ctr. Field Robotics, 2002
 - [12] Young-Ho Choi Tae-Kyeong Lee Se-Young Oh, "A line feature based SLAM with low grade range sensors using geometric constraints and active exploration for mobile robot", *Autonomous Robots*, 24: 13-27, 2008
 - [13] Christian P. Connette, Oliver Meister, Martin Hagele and Gert F. Trommer, "Decomposition of Line Segments into Corner and Statistical Grown Line Features in an EKF-SLAM Framework", *IEEE-RSJ, Intl. Conf. on Robots and Systems (IROS)*, 2007
 - [14] Andrea Garulli, Antonio Giannitrapani, Andrea Rossi and Antonio Vicino, "Mobile robot SLAM for line-based environment representation", *IEEE Conference on Decision and Control*, and the *European Control Conference*, 2005